MNRAS **000**, 1–5 (—) Preprint 5 March 2020 Compiled using MNRAS LaTeX style file v3.0

The GALAH Survey: Primordial lithium abundances measured in the atmospheres of warm dwarf stars

Xudong Gao[1,2★], Karin Lind[1,3], Anish M. Amarsi[1,4], Sven Buder[1,2], Joss Bland-Hawthorn[5,6], Simon W. Campbell[9], Martin Asplund[6,7], Andrew R. Casey[8,9], Ken C. Freeman[7], Geraint F. Lewis[5], Sarah L. Martell[6,10], Gayandhi M. De Silva[11], Jeffrey D. Simpson[10], Sanjib Sharma[5,6], Tomaž Zwitter[12], Daniel B. Zucker[6,11,13], Jonathan Horner[14], Ulisse Munari[15], Thomas Nordlander[6,7], Dennis Stello[5,6,10,16], Yuan-Sen Ting[17,18,19], Gregor Traven[20], Robert A. Wittenmyer[21] and the GALAH collaboration

[1] *Max-Planck-Institut für Astronomie, Königstuhl 17, D-69117 Heidelberg, Germany*
[2] *Fellow of the International Max Planck Research School for Astronomie & Cosmic Physics at the University of Heidelberg, Germany*
[3] *Department of Astronomy, Stockholm University, AlbaNova, Roslagstullbacken 21, SE-10691 Stockholm, Sweden*
[4] *Theoretical Astrophysics, Department of Physics and Astronomy, Uppsala University, Box 516, SE-751 20 Uppsala, Sweden*
[5] *Sydney Institute for Astronomy (SIfA), School of Physics, A28, The University of Sydney, NSW, 2006, Australia*
[6] *Center of Excellence for All-Sky Astrophysics in Three Dimensions (ASTRO-3D), Australia*
[7] *Research School of Astronomy & Astrophysics, Mount Stromlo*
Observatory, Australian National University, ACT 2611, Australia
[8] *Monash Centre for Astrophysics, Monash University, Clayton VIC 3800, Australia*
[9] *School of Physics and Astronomy, Monash University, Clayton VIC 3800, Australia*
[10] *School of Physics, University of New South Wales, Sydney, NSW 2052, Australia*
[11] *Department of Physics and Astronomy, Macquarie University, Sydney, NSW 2109, Australia*
[12] *Faculty of Mathematics and Physics, University of Ljubljana, Jadranska 19, 1000 Ljubljana, Slovenia*
[13] *Macquarie University Research Centre for Astronomy, Astrophysics & Astrophotonics, Sydney, NSW 2109, Australia*
[14] *University of Southern Queensland, Toowoomba, Queensland 4350, Australia*
[15] *INAF Astronomical Observatory of Padova, 36012 Asiago, Italy*
[16] *Stellar Astrophysics Centre, Department of Physics and Astronomy, Aarhus University, Denmark*
[17] *Institute for Advanced Study, Princeton, NJ 08540, USA*
[18] *Department of Astrophysical Sciences, Princeton University, Princeton, NJ 08544, USA*
[19] *Observatories of the Carnegie Institution of Washington, 813 Santa Barbara Street, Pasadena, CA 91101, USA*
[20] *Lund Observatory, Department of Astronomy and Theoretical Physics, Box 43, SE-221 00 Lund, Sweden*
[21] *University of Southern Queensland, Computational Engineering and Science Research Centre, Toowoomba, Queensland 4350, Australia*

Accepted —. Received —; in original form —

ABSTRACT

Lithium depletion and enrichment in the cosmos is not yet well understood. To help tighten constraints on stellar and Galactic evolution models, we present the largest high-resolution analysis of Li abundances A(Li) to date, with results for over 100 000 GALAH field stars spanning effective temperatures $5900\,\mathrm{K} \lesssim T_{\mathrm{eff}} \lesssim 7000\,\mathrm{K}$ and metallicities $-3 \lesssim \mathrm{[Fe/H]} \lesssim +0.5$. We separated the remaining stars into two groups, on the warm and cool side of the so-called Li-dip, a localised region of the Kiel diagram wherein lithium is severely depleted. We discovered that stars in these two groups show similar trends in the A(Li)-[Fe/H] plane, but with a roughly constant offset in A(Li) of 0.4 dex, the warm group having higher Li abundances. At $\mathrm{[Fe/H]} \gtrsim -0.5$, a significant increasing in Li abundance with increasing metallicity is evident in both groups, signalling the onset of significant Galactic production. At lower metallicity, stars in the cool group sit on the Spite plateau, showing a reduced lithium of around 0.4 dex relative to the primordial value predicted from Big Bang nucleosynthesis (BBN). However, stars in the warm group form an elevated plateau that is largely consistent with the BBN prediction. This may indicate that these stars in fact preserve the primordial Li produced in the early Universe.

Key words: stars: abundances — stars: atmospheres — stars: late-type — Galaxy: abundances — cosmology: primordial nucleosynthesis — techniques: spectroscopic

© — The Authors

1 INTRODUCTION

Lithium is a fragile element that can be destroyed by proton capture reactions at relatively low temperatures (~ 2.5×10^6 K) in stellar interiors (Pinsonneault 1997). Standard stellar evolution models suggest that the convective envelopes are weakly developed in low-mass unevolved (main-sequence) stars with effective temperatures ($T_{\rm eff}$) larger than 6000 K, thus precluding the surface Li from reaching the interior to be destroyed (Deliyannis et al. 1990). As such, the unevolved, metal-poor stars are expected to retain near-primordial Li abundances, providing an opportunity to put constraints on Big Bang nucleosynthesis (BBN). However, a significant difference has been found between the Li abundance measured from very metal-poor stars in the Galaxy that fall on the so-called “Spite plateau” at A(Li)[1] ≈ 2.2 (Spite & Spite 1982), and the prediction by standard BBN models A(Li) = 2.75 ± 0.02 (Pitrou et al. 2018). This is the well-known Cosmological Lithium Problem (Spite et al. 2012).

A striking feature called the "lithium dip" (Li-dip), was first observed in (Population I) main-sequence stars in the Hyades open cluster by Wallerstein et al. (1965), and later confirmed by Boesgaard & Tripicco (1986). Li abundances show a significant drop in the temperature range 6400 − 6850 K. Within this narrow temperature range, the depletion in A(Li) can reach a factor of 100 relative to stars out of this region. On the warm side of the Li-dip, the Li abundances increase sharply with increasing effective temperature. For $T_{\rm eff}$ larger than ~ 6900 K, the Li abundances seem to remain constant, compatible with the Galactic value (i.e., the meteoritic value; see Lodders et al. 2009). However, few abundance determinations are available for stars in this $T_{\rm eff}$ region, because the primary abundance diagnostic, the Li I 670.8 nm resonance line, is weaker in warmer stars; excessive line broadening due to typically fast stellar rotation further complicates spectroscopic analyses. On the cool side of the Li-dip, the Li abundances increase gradually with decreasing effective temperature until reaching a sort of plateau, which extends from ~ 6400 to ~ 6000 K. Stars in this region are slightly depleted in lithium, however this depletion is uniform, and is not nearly as severe as in the Li-dip stars.

Since the first observations, the presence of the Li-dip has also been found in many older star clusters, such as NGC 752 and M67 (Balachandran 1995), but not in the youngest open clusters (Boesgaard et al. 1988; Balachandran et al. 2011) – those with ages less than about 100 Myr. This indicates that the large lithium depletions that are now apparent in the Li-dip take place when the stars are on the main-sequence, rather than being there from the star’s birth, or occuring when the star was on the pre-main-sequence phase.

In order to meet observational constraints such as the complicated Li abundance behaviour observed in the main-sequence stars, several different non-standard stellar evolution models have been proposed, which take into consideration atomic diffusion (Michaud 1986) and rotation-induced mixing (Zahn 1992). However, these models cannot accurately account for the observed Li-dip. More recent works successfully managed to describe the Li-dip in young stellar cluster Hyades by also accounting for internal gravity waves (Montalbán & Schatzman 2000; Charbonnel & Talon 2005). According to their models, one can describe the Li-dip feature by characterising the stars into three groups based on temperature (Charbonnel & Talon 2005): those warmer than the Li-dip, those within the Li-dip, and those cooler. Stars in the warm group have the shallowest convective envelopes, making them nearly unaffected by diffusion and rotation-induced mixing. Li-dip stars experience rotational mixing as the convective envelope deepens, resulting in severe Li destruction. But for stars in the cool group, even though they have even deeper convective envelopes, internal gravity waves become activated and efficiently extract angular momentum from the interior; this counter-acts the rotational mixing, and limits the amount of lithium destruction. For these reasons, stars on either side of the Li-dip have mechanisms to prevent lithium destruction to different extents. In particular, the warm stars may allow us to probe the primordial Li abundance.

The Li-dip phenomenon has also been observed in unevolved field stars (e.g. Randich et al. 1999; Chen et al. 2001; Lambert & Reddy 2004; Ramírez et al. 2012; Bensby & Lind 2018; Aguilera-Gómez et al. 2018). These earlier studies have typical sample sizes of 200-2000 field stars in total, thus spanning only very limited ranges in stellar properties and containing very few stars on the warm side of the Li-dip. To study the lithium evolution comprehensively, a large sample of stars with homogeneous measurements is needed.

The aim of the present paper is to investigate the behaviour of lithium among late-type field stars including main-sequence, turn-off and early sub-giant phase. Using data from the Galactic Archeology with HERMES (GALAH) survey (De Silva et al. 2015), we present the largest sample of lithium abundances so far. The data span benefit from a homogeneous determination of stellar parameters and lithium abundances, and span a wide range of metallicities. These two aspects of our study allow us to draw fresh insights into the lithium puzzle.

2 OBSERVATIONS AND ANALYSIS

We observed over 650 000 FGK field stars in the solar neighbourhood as part of the GALAH (De Silva et al. 2015), K2-HERMES (Sharma et al. 2019) and TESS-HERMES (Sharma et al. 2017) spectroscopic surveys. The spectral resolving power of the surveys $R = \frac{\lambda}{\Delta\lambda} \approx 28\,000$ is sufficiently matched to the stellar absorption lines under study. To avoid stars with large convection-driven lithium depletion, we mainly target the dwarf and sub-giant stars with $T_{\rm eff}$ ranging from 5900 to 7000 K covering a large range of metallicity from [Fe/H] = +0.5 to [Fe/H] = −3.0, which includes the Spite plateau at the metal-poor end. After excluding spectroscopically resolved binaries, and observations with fitting inaccuracies, low signal-to-noise ratio, strong emission lines or reduction issues, we obtain a set of 62 945 stars with lithium detections and a separate set of 59 117 stars with upper limits on the Li abundance.

The stellar parameters $T_{\rm eff}$, [Fe/H], projected rotational velocities $v \sin \iota$, and line-of-sight radial velocity were determined simultaneously in a homogeneous way by fitting observed neutral and ionized lines of Sc, Ti, and Fe lines that are unblended and for which reliable atomic data are available, as well as the $T_{\rm eff}$-sensitive Hα and Hβ lines, using the GALAH analysis pipeline (Buder et al. 2018). Surface gravities were constrained consistently and simultaneously by the fundamental relation between the absolute magnitude, mass and $T_{\rm eff}$ (Buder et al. 2019). Stellar masses and ages were estimated by a Bayesian implementation of isochrone fitting (Lin et al. 2018). Having obtained the optimal stellar parameters, Li abundances were then derived using non-local thermodynamic equilibrium spectral synthesis (Gao et al. 2018) for the Li I 670.8 nm resonance line. The non-LTE departure coefficients come from the model described in (Lind et al. 2009).

---

[1] $A(\mathrm{Li}) = \log \frac{n_{\rm Li}}{n_{\rm H}} + 12$, where $n_{\rm Li}$ and $n_{\rm H}$ are the the number densities of lithium and hydrogen, respectively.

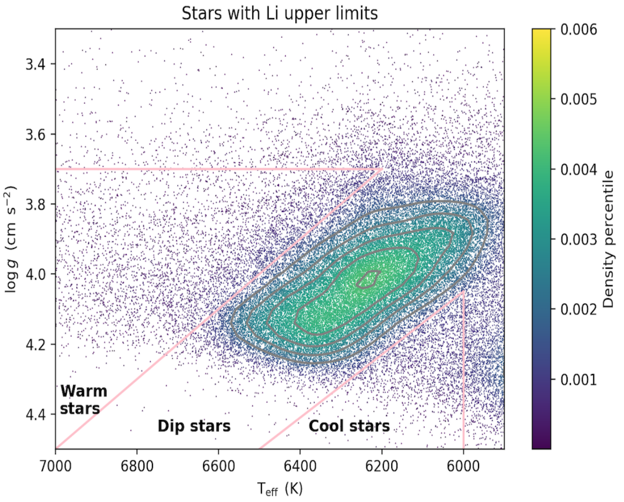
Stars with Li upper limits

Stars with Li detections

Figure 1. Loci of the sample stars with A(Li) upper limits and lithium detections in the $T_{\rm eff}$-log g panel, respectively. *Left panel*: Loci of stars with lithium upper limits (62 945 stars). The colour bar represents density distribution of stars, with bright colours implying high density. The contours that are overplotted, represent the density percentile of lithium upper limit stars. We define the approximate boundaries of the Li-dip region by using linear fits in the left and right edges of the outermost contour. The boxes that are located inside the pink triangles are classified as the warm group and cool group of stars, respectively. Stars that lie outside these three regions are removed from the comparison in Fig. 2. ***Right panel***: Loci of stars with lithium detections (59 117 stars)

In this work, we consider lithium to be detected when the line depression (*i.e.*, $D \equiv 1 - \frac{F_\lambda}{F_c}$) is deeper than 1.5σ of the flux error within the line mask, and at least 3% below the normalised continuum flux. In all other cases, the measurement is considered as an upper limit. We estimate upper limits on the Li abundance based on linear interpolation in four dimensions, using a large matrix that connects line strength with Li abundance, effective temperature, surface gravity, and rotational velocity.

3 RESULTS

Fig. 1 shows the locations of the sample stars with lithium detections and upper limits in the Kiel diagram, respectively. Comparing the two panels, a clear gap is seen in the distribution of stars for which lithium could be detected (Fig. 1b), whereas a significant overdensity of stars for which only upper limits on the Li abundance could be obtained is seen in the same region (Fig. 1a). Most of the stars with upper limits are concentrated in this diagonal region between $T_{\rm eff} \sim 6300$ to 6600 K, with surface gravity (log g) ranging from 3.8 to 4.3 dex. We interpret this as the Li-dip region: these stars have experienced severe lithium depletion and are now evolving towards to the sub-giant branch.

To characterise the Li-dip region in the Kiel diagram, we first narrow down the log g range of our sample (3.7 – 4.5 dex) to reduce the the evolutionary effects on lithium due to post-main-sequence stars. Our sample now consists of upper main-sequence stars, turn-off stars and early sub-giants. Moreover, we remove all the stars with $T_{\rm eff}$ less than 6000 K, as those cooler stars undergo strong and rapid lithium depletion, due to their larger convective envelopes (e.g. Bensby & Lind 2018). The density contours are then overplotted on the distribution of A(Li) upper limits. We define the approximate boundaries of the Li-dip region by using linear fits in the left and right edges of the outermost contour. We delineate the left and right boundaries of the Li-dip region as the warm group and cool group of stars, respectively.

The left panel of Fig. 2 shows lithium trends as a function of metallicity, for the warm and cool groups of stars. At low metallicity ([Fe/H] $\lesssim -1$ dex), the stars in the cool group have ages in excess of 11 Gyr and reveal the Spite Plateau, showing low and near-constant Li abundances. In contrast, there are no old, metal-poor warm stars in our sample: such stars have higher masses and have evolved off the main-sequence after such a long period. Thus the stars in the warm group only appear above [Fe/H] $\gtrsim -1.0$. Up to $-1.0 \lesssim$ [Fe/H] $\lesssim -0.5$, the warm group shows a similar constant lithium plateau, but elevated by almost three times that of the cool group (0.4 dex). We measure A(Li)= 2.69 ± 0.06. Remarkably, this plateau is largely consistent with the predictions of BBN (A(Li) = 2.75 ± 0.02). One interpretation of this, is that both Galactic enrichment and stellar destruction have been insignificant in this population of stars; in other words, that these stars in fact preserve the primordial Li produced in the early Universe.

At higher metallicities [Fe/H] $\gtrsim -0.5$, both the warm and cool groups of stars show an increasing trend in A(Li). This is probably caused by Galactic enrichment (Prantzos et al. 2017). It is interested to note that even in this metallicity regime, the difference in the average Li abundances between the warm and cool groups is still 0.4 dex, and remains so up to solar metallicity.

The right panel of Fig. 2 shows the corresponding location of warm and cool group stars in the Kiel diagram with color-coded Li abundances. There is a clear gradient in the Li abundances across the Kiel diagram, delineating the Li-dip from the warm and cool groups of stars. It shows that stars in the cool group are systematically more depleted in lithium than those in the warm group. Since most of our stars are centered around the solar metallicity, we overplotted the evolutionary tracks of different masses in solar metallicity on the distribution of our targets. The theoretical mod-

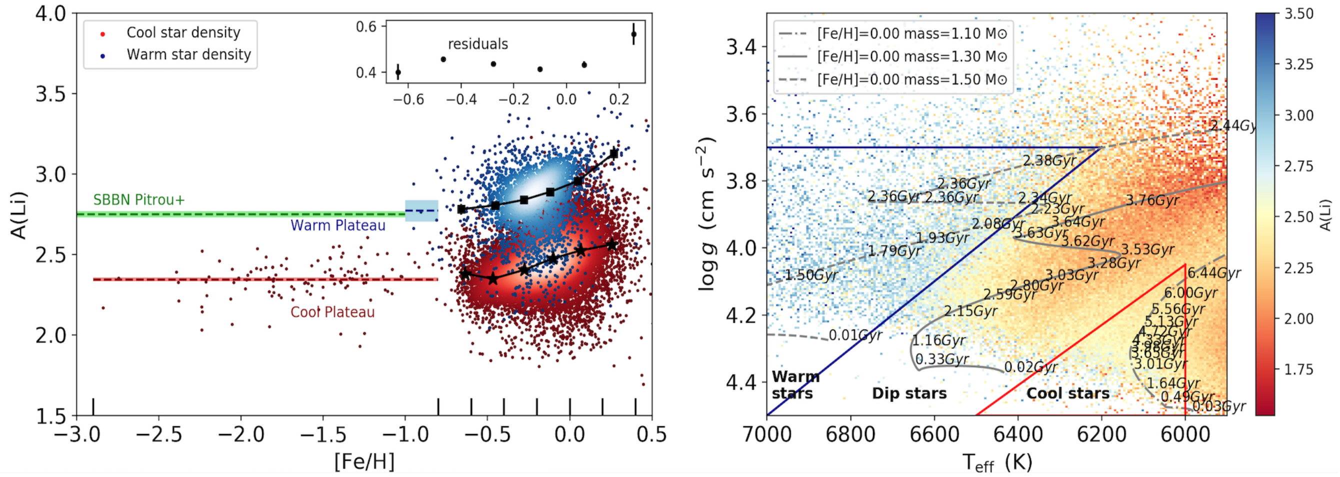

Figure 2. Lithium trends as a function of metallicity as observed for the warm and cool groups of stars. ***Left panel***: Observational data of lithium from the warm and cool groups as a function of [Fe/H]. Only detections are retained in each group and plotted as colour-coded density. Black squares and asterisks represent the median Li abundances of the corresponding metallicity bins (indicated with black lines above the bottom axis) in the warm and cool groups of stars, respectively. The error bars represent the uncertainties of the mean, most of them are too small to be shown. The residual of the mean Li abundances between the two groups in the corresponding metallicity range is shown as an inset in the upper right corner. The mean values of stars in the most metal-poor bin that stretches between $-2.9 < \mathrm{[Fe/H]} < -0.8$ are instead marked with blue and red dashed lines for the warm and cool groups of stars respectively, and marked as "Warm Plateau" and "Cool Plateau". The corresponding shaded areas represent the standard error of the mean. The primordial Li abundance from the standard BBN Pitrou et al. (2018) is shown with a green dashed line. ***Right panel***: All the stars with lithium detections and upper limits are colour-coded by A(Li) in the T_{eff}-log g panel. The corresponding location of the warm and cool groups of stars are shown in the blue and red boxes, respectively. The colour gradient of Li abundance clearly shows the lithium differences between the three regions. Evolutionary tracks of different masses in the solar metallicity are overplotted.

els support our speculation that we have captured the evolutionary track of Li-dip stars in our observations.

At a given [Fe/H], there is a difference in mean age between the warm group (young) and cool group (old), because of the sample selection method. The age difference is largest at low metallicity (up to 7 Gyr) and steadily decreases to become insignificant at the highest metallicities. The lower Li abundances of the cool group should thus be interpreted as a combined effect of their lower effective temperatures and older ages, making depletion more efficient and giving it longer time to act. The age difference may lead one to speculate that Galactic chemical evolution has elevated the initial Li abundances in the warm group compared to in the cool group. However, our data suggests that such enrichment scales with increasing metallicity and only becomes noticeable at $\mathrm{[Fe/H]} \gtrsim -0.5$. Recent observations of Li abundance in the low metallicity gas ($\mathrm{[Fe/H]} \sim -0.5$) of the Small Magellanic Cloud (Howk et al. 2012) and in warmer stars in the open cluster NGC 2243 (François et al. 2013) ($\mathrm{[Fe/H]} = -0.52$; an estimated age of 4.3 Gyr) are in good agreement with our A(Li) measurements in the warm group of stars. Thus, our data are consistent with the metal-poor stars of the warm group having primordial lithium abundances as predicted by BBN, without obvious Galactic lithium enrichment.

4 CONCLUSIONS

To reduce the complex behaviour of lithium in the field stars, for the first time we draw a comparison between the warm and cool groups of stars, which are located on the warm and cool side of the Li-dip, respectively. Here we find that Li abundances in the two groups show a similar pattern as a function of [Fe/H], however, stars in the cool group are more depleted in lithium than those in the warm group by a factor of three. This difference is determined from more than 100 000 stars that have a wide range of stellar properties and chemistry. The implications we can obtain from this result are as follows.

- We find that at $\mathrm{[Fe/H]} \lesssim -0.5$, the average Li abundance of stars warmer than the Li-dip is consistent with the primordial lithium abundance as predicted by BBN. Since Galactic production of lithium has not yet broken the Spite plateau in this metallicity regime, we suggest that the atmospheres of the stars in the warm group have indeed preserved the primordial lithium abundance. This lends strong empirical support to the standard cosmological model of the early universe.
- We infer that, at a given metallicity, the three different regimes (warm, Li-dip, cool) follow different lithium depletion mechanisms. For the stars in the cool group, the depletion is not strongly dependent of metallicity; instead it is primarily governed by a star's main-sequence temperature and age. How much lithium has been depleted is a combination of temperature and stellar age, causing a near-constant offset with respect to the warm group.
- We identify $\mathrm{[Fe/H]} \approx -0.5$ as the turning point where the Li abundances break the plateau and Galactic lithium production becomes significant. We see this in both the warm and the cool groups of stars. Given that the Spite plateau stars (of the cool group) have already experienced a large depletion of lithium and therefore do not reflect the true primordial value, we recommend that modellers apply the BBN-predicted Li abundance, instead of the Spite plateau (Spite & Spite 1982) Li abundance, as the initial value in chemical evolution models (Prantzos 2012; Prantzos et al. 2017).

ACKNOWLEDGEMENTS

XDG, KL, AMA and SB acknowledge funds from the Alexander von Humboldt Foundation in the framework of the Sofja Kovalevskaja Award endowed by the Federal Ministry of Education and Research, and KL also acknowledges funds from the Swedish Research Council (grant 2015-004153) and Marie Skłodowska Curie Actions (cofund project INCA 600398). TZ acknowledges financial support of the Slovenian Research Agency (research core funding No. P1-0188). SLM and JDS acknowledges the support of the Australian Research Council through Discovery Project grant DP180101791. Parts of this research were conducted by the Australian Research Council Centre of Excellence for All Sky Astrophysics in 3 Dimensions (ASTRO 3D), through project number CE170100013. YST is grateful to be supported by the NASA Hubble Fellowship grant HST-HF2-51425 awarded by the Space Telescope Science Institute. SWC acknowledges federal funding from the Australian Research Council though the Future Fellowship grant entitled 'Where are the Convective Boundaries in Stars?' (FT160100046). This work is also based on data acquired from the Anglo-Australian Telescope. We acknowledge the traditional owners of the land on which the AAT stands, the Gamilaraay people, and pay our respects to elders past and present.

REFERENCES

Aguilera-Gómez C., Ramírez I., Chanamé J., 2018, A&A, 614, A55
Balachandran S., 1995, ApJ, 446, 203
Balachandran S. C., Mallik S. V., Lambert D. L., 2011, MNRAS, 410, 2526
Bensby T., Lind K., 2018, A&A, 615, A151
Boesgaard A. M., Tripicco M. J., 1986, ApJ, 302, L49
Boesgaard A. M., Budge K. G., Ramsay M. E., 1988, ApJ, 327, 389
Buder S., et al., 2018, MNRAS, 478, 4513
Buder S., et al., 2019, A&A, 624, A19
Charbonnel C., Talon S., 2005, in Alecian G., Richard O., Vauclair S., eds, EAS Publications Series Vol. 17, EAS Publications Series. pp 167–176, doi:10.1051/eas:2005111
Chen Y. Q., Nissen P. E., Benoni T., Zhao G., 2001, A&A, 371, 943
De Silva G. M., et al., 2015, MNRAS, 449, 2604
Deliyannis C. P., Demarque P., Kawaler S. D., 1990, ApJS, 73, 21
François P., Pasquini L., Biazzo K., Bonifacio P., Palsa R., 2013, A&A, 552, A136
Gao X., et al., 2018, MNRAS, 481, 2666
Howk J. C., Lehner N., Fields B. D., Mathews G. J., 2012, Nature, 489, 121
Lambert D. L., Reddy B. E., 2004, MNRAS, 349, 757
Lin J., Dotter A., Ting Y.-S., Asplund M., 2018, MNRAS, 477, 2966
Lind K., Asplund M., Barklem P. S., 2009, A&A, 503, 541
Lodders K., Palme H., Gail H.-P., 2009, Landolt Börnstein, p. 712
Michaud G., 1986, ApJ, 302, 650
Montalbán J., Schatzman E., 2000, A&A, 354, 943
Pinsonneault M., 1997, ARA&A, 35, 557
Pitrou C., Coc A., Uzan J.-P., Vangioni E., 2018, Physics Reports, 754, 1
Prantzos N., 2012, A&A, 542, A67
Prantzos N., de Laverny P., Guiglion G., Recio-Blanco A., Worley C. C., 2017, A&A, 606, A132
Ramírez I., Fish J. R., Lambert D. L., Allende Prieto C., 2012, ApJ, 756, 46
Randich S., Gratton R., Pallavicini R., Pasquini L., Carretta E., 1999, A&A, 348, 487
Sharma S., et al., 2017, preprint, (`arXiv:1707.05753`)
Sharma S., et al., 2019, arXiv e-prints,
Spite F., Spite M., 1982, A&A, 115, 357
Spite M., Spite F., Bonifacio P., 2012, Memorie della Societa Astronomica Italiana Supplementi, 22, 9
Wallerstein G., Herbig G. H., Conti P. S., 1965, ApJ, 141, 610
Zahn J.-P., 1992, A&A, 265, 115